Analytical Evaluation of Chunk-Based Tractable Multi-Cell OFDMA System

Pillappan KAVITHA, Sethu SHANMUGAVEL

Dept. of ECE, National Engineering College, Kovilpatti, Tamil Nadu 628 503, India

kavitha@nec.edu.in, sethusvel@gmail.com

Submitted May 6, 2017 / Accepted September 14, 2017

Abstract. *This paper evaluates thoroughly the performance of multi-cell OFDMA system. The two types of deployment in multi-cell OFDMA system, such as Strict Fractional Frequency Reuse (FFR) and Soft FFR (SFR) were evaluated. In order to model the base station locations, homogeneous Poisson point processes were used, i.e. tractable model instead of hexagonal grid was considered. In order to reduce complexity, chunk-based resource allocation scheme was embedded. Each cell divides the users into the users of the central cell area and the users of the cell edge area according to their average received Signal to Interference and Noise Ratio (SINR) compared with FFR threshold. The primary stage of the analysis includes the spectral efficiency's expression deriving from these two deployment scenarios, followed by the analysis with the use of coverage probability. However, the improvement of spectral efficiency is achieved in the case of SFR. On the contrary, coverage probability is far improved by using strict FFR scheme. Through numerical anaysis, We have shown that the optimal FFR threshold to achieve the highest spectral efficiency was 12 dB for both Strict FFR as well as SFR.*

Keywords

Chunk, spectral efficiency, coverage probability, Multi-Cell OFDMA, resource allocation, frequency reuse, Poisson model

1. Introduction

Long Term Evolution (LTE) as well as LTE Advanced systems considered Orthogonal Frequency Division Multiplexing (OFDM) for downlink radio transmission due to wideband transmission. As an advanced multiple access technique, OFDM-based Orthogonal Frequency Division Multiple access (OFDMA) i.e. an extension of OFDM, has become very promising high data rate wireless communications which provides multiple users transmissions by dynamically allocating radio resources to different users. OFDMA offers nearly null intra-cell interference due to orthogonality among the subcarriers. However, inter-cell interference is a major bottleneck in multi-cell environment particularly for the edge users in the cell. This occurs when frequency reuse is employed in order to increase spectral efficiency [1].

In [2], the authors investigated that by properly allocating the radio resources to a Radio Network Controller (RNC) and base stations (BSs), no intra-cell interference can be obtained. In [3], the authors summarized the impact of co-existence between advanced communication systems due to the use of the same frequency band for multimedia applications. In [4], the authors discussed co-channel existence between LTE and WLAN services in the ISM band. In [5], the authors addressed the problem of assigning subchannels in a OFDMA based multi-cell downlink underlay Cognitive Radio Networks (CRN).

FFR resource allocation reduces inter-cell interference as well as it improves spectral efficiency [6]. In [7], to improve the trunking gain, the authors proposed dynamic resource allocation scheme. To allocate resources among the base stations, either full co-ordination or frequency reuse between the base stations may be considered to mitigate inter-cell interference. But in [8], the authors proved that full co-ordination between the base stations provide more efficiency than frequency reuse for dynamic SINR-based strict FFR.

To reduce complexity in the single subcarrier-based allocation, the correlation between adjacent subcarriers in the OFDM systems can be considered. When the channel conditions are affecting (bad condition) or not affecting (good condition) a subcarrier, then its adjacent subcarriers are most likely to be affected in a similar way. Thus, properly grouping a set of contiguous OFDM subcarriers into one chunk and the resources may be allocated as chunk instead of subcarriers in resource allocation [9]. Chunk can be allocated according to Signal to Noise Ratio (SNR) or Bit Error Rate (BER) constraint. In paper [10], the authors analytically studied the performance of BER-based chunk allocation and compared the performance with SNR-based allocation. They proved that BER-based chunk allocation gives better performance than the later. In [11], chunk-based resource allocation was proposed for Multiple Input Single Output (MISO)-OFDMA Distributed Antenna System (DAS) in order to reduce the implementation complexity in downlink. In [12], in addition

to chunk allocation, joint power and bit allocation scheme were proposed with BER constraint.

In [13], the authors proposed chunk-based subcarrier assignment. Here, proportional fairness scheduling, i.e. instead of assigning subcarrier of chunk to the user with the highest channel gain, assigning the chunk to the user with the highest requested rate relative to the average user rate was considered. They proved that this method outperforms the adaptive resource allocation with proportional rate constraints [14]. After performing subcarrier assignment, power is assigned to the corresponding subcarriers. In paper [15], they proposed a reduced-power channel reuse (RPCR) scheme in order to improve the capture failure problem. In order to reduce implementation cost and the adverse impact of imperfect power control, the power level at the different cells is determined a priori and is static. Since it is difficult to obtain accurate channel and interference measurements of bursty data traffic for determining appropriate values of transmission power, they have shown that this method is an attractive one.

In chunk-based subcarrier assignment, due to grouping of adjacent sucarriers results in Peak to Average Power Ratio (PAPR) problem. In [16], Partial Transmit Sequence(PTS) techniques have been proposed to reduce PAPR. In [17], the authors proposed the two techniques such as soft reduction combined with μ-law (μLSR) and subtracting cyclic prefix output from μ-law output (μLaCP) to reduce PAPR without BER deterioration. In [18], μLSR and μLaCP techniques have been used for Turbo coded OFDM system. The same transmit-power can be allocated for all the subcarriers within a chunk [19].

In order to improve the spectral efficiency, modulation parameters are adapted under different constellation restrictions and BER constraints [20]. In [10–12], the chunk-based resource allocation performances have been analyzed only in a single cell environment. Based on actual users measurements or existing propagation studies or simulations, initial/recommended operational configurations to be applied along with the selected static ICIC strategy, either SFR or FFR is considered in [21]. In [22], the performance of chunk-based resource allocation has been analyzed in multi-cell OFDMA system in conjunction with FFR concept. Also, they investigated the optimal radius ratio of central area to the whole cell area to achieve highest spectral efficiency. In [22], the base stations are modelled as hexagonal layout.

In [23], the authors described how wireless networks are analyzed using stochastic geometry and random graph theory. In [24], [25] SINR distribution has been obtained for tractable model, i.e. the base stations are modelled using homogeneous Poisson point process (PPP). They did not include FFR concept in multi-cell system. In [26], the performance of coverage probability and average rate in Strict FFR and SFR systems have been analytically evaluated for tractable base station model. Here, they did not consider the dynamic coordination among base stations. In [27], the authors derived an expression for spectral efficiency of OFDMA transmission in the presence of users and Carrier Frequency Offset (CFO). Also, they compared the performance of OFDMA and Multi Carrier-Code Division Multiple Access (MC-CDMA) and proved that OFDMA offers higher spectral efficiency than MC-CDMA under high load conditions which is normally experienced at peak hours and dense areas.

The main contribution of this paper is to analyze the spectral efficiency for tractable model using base station cooperation in conjunction with chunk-based resource allocation and also to investigate the optimal FFR threshold γ_{TH}, i.e. the parameter which is used to split the user into the users of the central cell area and the users of the cell edge area to achieve the highest spectral efficiency.

The paper is organized as follows. Section 2 describes the system model. Section 3 analyses the average spectral efficiency. Section 4 discusses its numerical result. The paper concludes in Sec. 5.

2. System Model

We consider an OFDMA cellular downlink. Reference to the literature preferred in which the PPP model is described and analysed for base station locations [24–27].

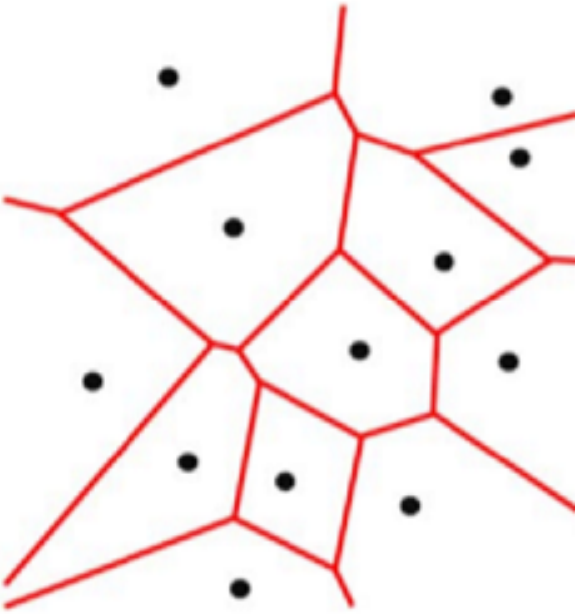

Fig. 1. Construction of Voronoi diagram.

The algorithm steps for the irregular cellular layout construction are described below.

- Step 1: Base stations locations are distributed as a spatial PPP [28].
- Step 2: Lines are drawn in between the mid point of each base station location and its adjacent base station locations.
- Step 3:Intersection of lines around each base station is taken as vertices of the corresponding cell.

- Step 4: Vertices are connected and considered as a cell with unequal coverage area. Voronoi diagram construction is shown in Fig. 1.

Zoomed out portion of 15×5 km^2 area of irregular cellular layout with 20 cells for FFR and SFR deployments are shown in Fig. 2 and 3, respectively. Since we use PPP to distribute base station locations, each cell covers different cell area or shape, i.e. coverage area of all cells is not equal. Geographic interpretation of this cell is different from regular hexagonal cell layout. Each cell is divided into the central cell area and the cell edge area according to the predefined threshold, i.e. FFR threshold (γ_{TH}). Thus, the FFR threshold (γ_{TH}) for irregular layout is a design parameter similar to the interior radius of hexagonal layout.

In graph theory, graph colouring is an assignment of colors to certain objects in a graph. The main property of graph colouring is to assign the colours to vertices where the no two adjacent vertices will have same colours. Here, assignment of colors corresponds to frequency band allocation. So, in this paper, graph colouring theory has been used to divide the available frequency bands among the multiple base stations. The same frequency can be reused among the areas with the same colour. From four colour theorem [29], in order to ensure the no two adjacent base station cell edge area users will have the same frequency band, the minimum number of the frequency bands required to avoid the interference in the users of the cell edge area is 4. So, the whole available frequency bands are divided into five frequency bands as shown in the Fig. 2. Four frequency bands are allocated to all the users of the cell edge area, whereas one frequency band is allocated to the users of the central cell area of all cells.

But in soft FFR, frequency bands are divided into four. In SFR, the frequency bands allocated to the users of the central cell area of one cell are shared by the users of the cell edge area of the adjacent cell in order to utilize the spectrum efficiently than FFR. Therefore, for strict FFR the frequency reuse factor in the central cell area is 1 due to the use of the same frequency band for all central cell area users, but for the cell edge area it is 1/4, i.e. out of 4 cells in a cluster one cell uses that particular frequency band. For SFR, the frequency reuse factor in the central cell area as well as the cell edge area is 2/4, i.e. out of 4 cells in a cluster two cells use that particular frequency band. The reference cell is marked as capital R inside the cell, i.e. the cell nearest to the origin. One of the users in the cell is considered as the reference user. Reference user is denoted as big dot in reference cell and the users positions are denoted as small dots.

Chunks may be allocated to the users of the central cell area or the users of the cell edge area according to the channel condition. From Fig. 2 for Strict FFR, if the chunk is allocated to the users of the central cell area in the reference cell, then the same chunk is allocated to the users of the central cell area of all cells through the base station co-ordination. Then the users in the central cell area receive interference

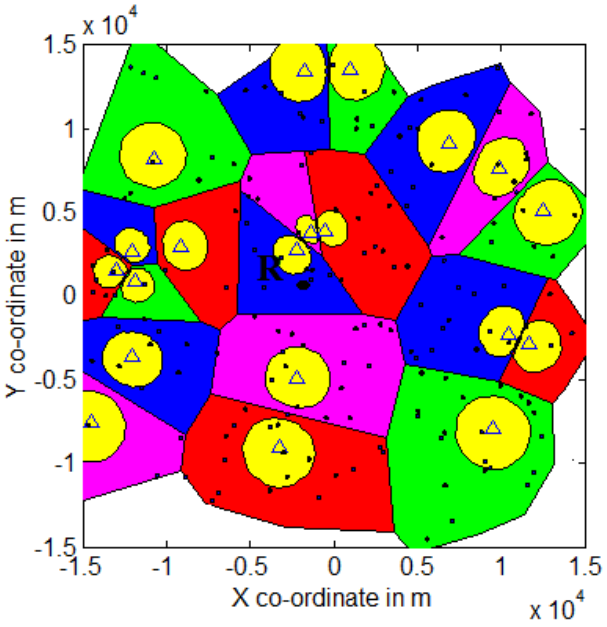

Fig. 2. Illustration of base station FFR deployment using Poisson point process.

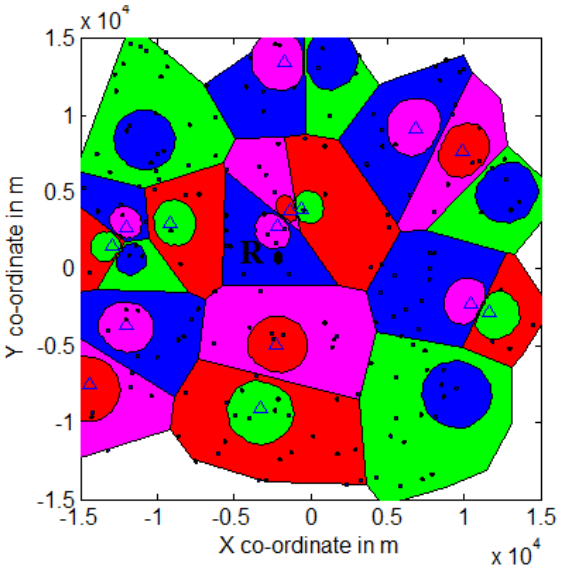

Fig. 3. Illustration of base station SFR deployment using Poisson point process.

from all remaining 19 base stations. If the chunk is allocated to the users of the cell edge area in the reference cell, then the same chunk is allocated to the users of the cell edge area of the remaining five blue cells. Then, the users in the cell edge area receive interference only from five base stations.

From Fig. 3 for SFR, if the chunk is allocated to the central cell user of the reference cell, then the same chunk is allocated to the users of the central cell area of blue cells as well as the users of the cell edge area of red cells through the base station co-ordination. Then, the users in the central cell area receive interference from the corresponding base stations. If the chunk is allocated to the users of the cell

edge area in the reference cell, then the same chunk is allocated to the users of the cell edge area as well as the users of the central cell area. Then, the users in the cell edge area receive interference from the corresponding base stations. Unlike hexagonal layout, it receives unequal amount of total interference power from all the base stations according to the location, i.e. users nearer to the base station may receive more interference power than the users far away from the base station due to the irregularly placed base stations. Here, the users in the cell are divided into the users of the central cell area and the users of the cell edge area according to the average received SINR of the user. Base station classifies users as the central cell area frequency band user or the cell edge area frequency band user. If the average received SINR of the user is greater than FFR threshold (γ_{TH}), then that users will use the frequency allocated to the central cell area and vice versa. FFR threshold (γ_{TH}) is a design parameter like radius in regular cell.

In OFDMA system, Rayleigh fading is assumed for each sub channel between any base station and the user of the reference cell. This is due to absence of line-of-sight path. But if there is a primary line of sight path, Rician fading is taken into account and performance of Rician fading used to be better than Rayleigh fading assumption. Moreover, noise is an Additive White Gaussian Noise (AWGN) with single sided power spectral density of N_0. The frequency response, $g_{k,n,l}$ of the l^{th} sub channel between the base station (BS)k, and the n^{th} user can be defined by the combination of path loss, fading, and phase. It is given by [22]

$$g_{k,n,l} = d_{k,n}^{-\alpha/2} h_{k,n,l} \mathrm{e}^{\mathrm{j}\psi_{k,n,l}} \tag{1}$$

where α is the path loss exponent.The received power used to be proportional to $d_{k,n}^{-\alpha}$ due to the magnitude square of the frequency response of the channel. So, the frequency response of the channel is taken to be proportional $d_{k,n}^{-\alpha/2}$, $h_{k,n,l}$ is the magnitude of the channel fading of l^{th} sub channel between BS_k and n^{th} user, and is independent identically Rayleigh distributed with unitary mean square, $E(h_{k,n,l}^2)$, for all (k, n). $\psi_{k,n,l}$ is the channel phase and is assumed to be uniformly distributed in [0,2Π). Therefore, $g_{k,n,l}$ is identically and independently complex Gaussian distributed with zero mean for all k and n. Its variance is equal to the path loss, i.e. $\mathrm{E}(|g_{k,n,l}|^2) = d_{k,}^{-\alpha}$. Due to different transmission distances, frequency responses of different users have different variances. Although variances are different, fairness is provided through considering normalized received power. That is, the normalized power is given by, $\tilde{g}_{k,n,l} = g_{k,n,l}/d_{k,n}^{-\alpha/2} = h_{k,n,l}.\mathrm{e}^{\mathrm{j}\psi_{k,n,l}}$.

In subcarrier based resource allocation, the subcarrier is allocated according to the channel condition. If the number subcarriers required to be allocated is high, for each subcarrier the channel condition has to be checked. This increases the complexity in resource allocation. In order to reduce the complexity in resource allocation, consecutive M sub channels, i.e. $\hat{g}_{k,n,q} = [\tilde{g}_{k,n,(l-1)M+1}, \ldots, \tilde{g}_{k,n,lM}]$ are grouped together to form chunk using correlation among adjacent subcarriers in the chunk-based resource allocation. This reduces the complexity by the number of subcarriers within the chunk, i.e. M. The channel fading of the chunk is defined by the average channel fading of all sub channels within the chunk, and is given by [22]

$$\hat{h}_{k,n,q} = \left(\frac{\hat{g}_{k,n,q} \hat{g}_{k,n,q}^{\mathrm{H}}}{M} \right)^{1/2},$$

$$\hat{h}_{k,n,q} = \left(\frac{\tilde{g}_{k,n,(l-1)M+1}^2 + \tilde{g}_{k,n,(l-1)M+2}^2 + \ldots, + \tilde{g}_{k,n,lM}^2}{M} \right)^{1/2} \tag{2}$$

where $(.)^{\mathrm{H}}$ stands for the Hermitian conjugate, and $\hat{g}_{k,n,q}$ represents the frequency response vector q^{th} chunk of n^{th} user in the k^{th} cell. Equation (2) contains square terms. This effect has been cancelled by taking square root for an entire expression.

According to the average channel fading of all sub channels, the modulation scheme is adopted in order to improve the throughput [20]. But, the modulation scheme used in all subcarriers within one chunk is considered to be constant irrespective of the individual sub channel condition. Here, L-ary QAM modulation scheme was chosen. The following values are chosen for L, such as $L = 0, 2^2, \ldots, 2^b, \ldots, 2^B$, where b takes the values of even numbers and it represents the total number of bits per symbol. The data rate for the particular carrier is given by $r = \log_2(L)$.

3. Resource Allocation for Tractable Cellular OFDMA System

In this paper, the chunk allocation information is shared globally among all the base stations through base station coordination. For strict FFR, if the chunk is allocated to the users of the central cell area of the reference cell, then it receives the co-channel interference from the remaining 19 cells. If the chunk is allocated to the cell edge area user of the reference cell, then it receives the co-channel interference from the remaining five blue cells. For SFR, if the chunk is allocated to the users of the central cell area, then it receives the co-channel interference from four magenta cells as well as five remaining blue cells. If the chunk is allocated to the cell edge area user of the reference cell, it receives the co-channel interference from the remaining five blue cells as well as five green cells. The chunk is allocated according to the channel condition irrespective of the user location, i.e. either user belongs to the central cell area or the cell edge area. Fairness is considered among the users, i.e. the chunk allocation is not fixed. The channel with best condition may be either allocated to the central cell area users or the cell edge area users, i.e. all the users are considered equally.

Therefore, the q^{th} chunk is allocated to the n^{th} user in the reference cell when the following condition satisfies [22]

$$n_q = \arg \max_{1 \le n \le N} \left[\hat{h}_{1,n,q}^2 \right]. \tag{3}$$

After allocating the chunk to the user, the transmit power is allocated. The transmit chunk-power per subcarrier for the central cell area is denoted as P_c, and that for the cell edge area is denoted as P_e. If the q^{th} chunk is allocated to the n^{th} user of the reference first cell, the power of the received desired signal is given by

$$P_{S_n} = \begin{cases} P_c \hat{h}^2_{1,n,q} x^{-\alpha}, & \text{central cell area users,} \\ P_e \hat{h}^2_{1,n,q} x^{-\alpha}, & \text{cell edge area users} \end{cases} \quad (4)$$

where x is the distance between BS_1 and n^{th} user. Since, the number of interfering base stations is much larger than one, Gaussian approximation can be applied to the total co-channel interference from the other base stations. This approximation follows from the central limit theorem and the law of large number. So, the total co-channel interference component can be approximated as a Gaussian random variable. The variance of the total received co-channel interference component is given by

$$\eta^2_{I_n} = \begin{cases} E\left(\sum_{i\in I} P_c \hat{h}^2_{i,n,q} d^{-\alpha}_{i,n}\right), & \text{for FFR,} \\ E\left(\sum_{i\in I_c} P_c \hat{h}^2_{i,n,q} d^{-\alpha}_{i,n} + \sum_{i\in I_e} P_e \hat{h}^2_{i,n,q} d^{-\alpha}_{i,n}\right), & \text{for SFR,} \end{cases} \quad (5)$$

$$\eta^2_{I_n} = \begin{cases} E\left(\sum_{i\in I} P_c d^{-\alpha}_{i,n}\right), & \text{for FFR,} \\ E\left(\sum_{i\in I_c} P_c d^{-\alpha}_{i,n} + \sum_{i\in I_e} P_e d^{-\alpha}_{i,n}\right), & \text{for SFR} \end{cases} \quad (6)$$

where I represents the interfering base stations corresponding to strict FFR, and I_c and I_e represent interfering base stations transmitting in the same band to the users of the central cell area and the users of the cell edge area respectively.

Therefore, the instantaneous SINR of q^{th} chunk for n^{th} user,$\gamma_{n,q}(x_n, \theta_n)$, can be given as

$$\gamma_{n,q}(x_n, \theta_n) = \frac{P_{S_n}}{\eta^2_{I_n} + \eta^2} \quad (7)$$

where η^2 is the noise variance of the particular chunk.

4. Performance Analysis

The performance of the spectral efficiency in the chunk-based resource allocation scheme is analysed in this section for irregular tractable multi-cell OFDMA environment. Also, this section investigates the optimal FFR threshold γ_{TH} to achieve the highest spectral efficiency. This section analyses the performance of strict FFR scheme as well as soft FFR scheme. Then, trade-off analysis with the coverage probability is performed.

As shown in Fig. 2, the frequency reuse factor, denoted as ϵ_c, in the central cell area of a cell is one (i.e. $\epsilon_c = 1$), the same frequency in their central cell area is used by all the the users of the central cell area. But in the cell edge area, the frequency reuse factor, denoted as $\epsilon_e = 1/4$, i.e. cluster contains four frequency bands.

Therefore, the spectral efficiency of the n^{th} user on the q^{th} chunk, $C_{n,q}$, defined as the achievable bits per symbol, is given by

$$C_{n,q} = \begin{cases} \epsilon_c r_{n,q}(x_n, \theta_n), & \text{for the central cell area,} \\ \epsilon_e r_{n,q}(x_n, \theta_n), & \text{for the cell edge area} \end{cases} \quad (8)$$

where $r_{n,q}(x_n, \theta_n)$ is the data rate for n^{th} user on the q^{th} chunk. The data rate is chosen to satisfy the BER constraint of 10^{-3} with adaptive QAM modulation scheme [22]. Also, chunk is allocated to the user with best channel conditions.

4.1 Strict FFR Average Spectral Efficiency Analysis

The probability of allocating the q^{th} chunk to the central cell area is the same as the probability that the frequency reuse factor $\epsilon(q)$ is equal to $\epsilon_c = 1$, i.e. $P(\epsilon(q) = \epsilon_c = 1)$. The probability of the spectral efficiency for strict FFR is given by

$$P(C_S(q) = C) = \begin{matrix} P(\epsilon(q) = \epsilon_c) P(C_c(q) = C \mid \epsilon(q) = \epsilon_c) + \\ P(\epsilon(q) = \epsilon_e) P(C_e(q) = C \mid \epsilon(q) = \epsilon_e) \end{matrix}$$

$$P(C_S(q) = C) = \begin{matrix} P(\epsilon(q) = 1) P(C_c(q) = C \mid \epsilon(q) = 1) + \\ P(\epsilon(q) = 1/4) P(C_e(q) = C \mid \epsilon(q) = 1/4) \end{matrix} \quad (9)$$

where $P(\epsilon(q) = \epsilon_c) = P(\epsilon(q) = 1)$ is the probability that the q^{th} chunk is assigned to a user in the central cell area, an $P(\epsilon(q) = \epsilon_e) = P(\epsilon(q) = 1/4) = 1 - P(\epsilon(q) = \epsilon_c)$. $P(C_c(q) = C \mid \epsilon(q) = \epsilon_c)$ and $P(C_e(q) = C \mid \epsilon(q) = \epsilon_e)$ are the conditional spectral efficiencies of the chunk allocated to the users of the central cell area and the users of the cell edge area respectively.

Due to the statistically independent chunk channels fading of the users within the cell, each user has the equal probability to be assigned with the corresponding chunk, regardless of user location. Suppose, the number of users in the k^{th} cell is N_k and among N_k users, N_{kc} users are in the central cell area. Then, the conditional probability of chunk to be assigned to the users of the central cell area, $P(\epsilon(q) = \epsilon_c \mid N_{kc})$ is proportional to the ratio of N_{kc} to N_k is given by

$$P(\epsilon(q) = \epsilon_c \mid N_{kc}) = N_{kc}/N_k. \quad (10)$$

From the Appendix A, the probability of assigning a q^{th} chunk to the central cell area is given by

$$P(\epsilon(q) = \epsilon_c) = 1 - \exp\left(-\pi\lambda \left[\frac{P}{\gamma_{TH}(\sum_{i\in I} P_c d^{-\alpha}_{i,n} + \eta^2)}\right]^{\frac{2}{\alpha}}\right). \quad (11)$$

Similarly, the probability of assigning a q^{th} chunk to the cell edge area is given by

$$P(\epsilon(q) = \epsilon_e) = \exp\left(-\pi\lambda \left[\frac{P}{\gamma_{TH}(\sum_{i\in I} P_c d^{-\alpha}_{i,n} + \eta^2)}\right]^{\frac{2}{\alpha}}\right). \quad (12)$$

From [22], the probabilities $P(C_c(q) = C \mid \epsilon(q) = \epsilon_c)$ and $P(C_e(q) = C \mid \epsilon(q) = \epsilon_e)$ are described as

$$P(C_c(q) = C \mid \epsilon(q) = \epsilon_c) = \begin{cases} 1 - P(C_c(q) < B \mid \epsilon(q) = \epsilon_c), & C = B, \\ P(C_c(q) < C + 2 \mid \epsilon(q) = \epsilon_c) - \\ P(C_c(q) < C \mid \epsilon(q) = \epsilon_c, & \text{if C is even,} \\ 0 & \text{otherwise.} \end{cases} \quad (13)$$

$$P(C_e(q) = C \mid \epsilon(q) = \epsilon_e) = \begin{cases} 1 - P(C_e(q) < \frac{B}{4} \mid \epsilon(q) = \epsilon_e), & C = B, \\ P(C_e(q) < \frac{C+2}{4} \mid \epsilon(q) = \epsilon_e) - \\ P(C_e(q) < C \mid \epsilon(q) = \epsilon_e, & \text{if C is even,} \\ 0 & \text{otherwise.} \end{cases} \quad (14)$$

From Appendix B, the conditional spectral efficiencies $P(C_c(q) < C \mid \epsilon(q) = \epsilon_c)$ and $P(C_e(q) < C \mid \epsilon(q) = \epsilon_e)$ are given as

$$\begin{aligned} &P(C_c(q) < C \mid \epsilon(q) = \epsilon_c) \\ &= \int_0^\infty P(C_c(q) < C \mid x) f_X(x)\, \mathrm{d}x \\ &= \sum_{i=1}^{M} \rho_i \left(1 - \int_0^\infty \exp\left(T_c \eta^2 \nu^{\frac{\alpha}{2}} - 2\pi\lambda\beta\left(T_c, \alpha\right)\right)\right) \mathrm{d}\nu. \end{aligned} \quad (15)$$

This equation consists of incomplete gamma function. So, closed form does not exist. But integrals are easily evaluated and similarly,

$$\begin{aligned} &P(C_e(q) < C \mid \epsilon(q) = \epsilon_e) \\ &= \int_0^\infty P(C_e(q) < C \mid x) f_X(x)\, \mathrm{d}x \\ &= \sum_{i=1}^{M} \rho_i \left(1 - \int_0^\infty \exp\left(T_e \eta^2 \nu^{\frac{\alpha}{2}} - 2\pi\lambda\beta\left(T_e, \alpha\right)\right)\right) \mathrm{d}\nu \end{aligned} \quad (16)$$

Finally, the average spectral efficiency per chunk can be calculated by taking average over all the cells as well as chunks.

4.2 Soft FFR Average Spectral Efficiency Analysis

The probability of assigning the chunk to the user in the central cell area or the cell edge area is the same as that of strict FFR. But the interference is different due to the share of spectrum by the users of the central cell area as well as the users of the cell edge area.

$P(C_c(q) < C \mid x) = P(C_e(q) < C \mid x) = P\left(r_{n_q,q}\left(x_{n_q}, \theta_{n_q}\right) < \frac{4}{2}C \mid x\right)$.

So, from Appendix B,

$$\begin{aligned} &P(C_c(q) < C \mid x) \\ &= \sum_{i=1}^{M} \rho_i \left(1 - \int_0^\infty \exp\left(T_c \eta^2 \nu^{\frac{\alpha}{2}} - 2\pi\lambda\beta\left(T_c, \alpha\right)\right)\right) \mathrm{d}\nu, \end{aligned} \quad (17)$$

$$\begin{aligned} &P(C_e(q) < C \mid x) \\ &= \sum_{i=1}^{M} \rho_i \left(1 - \int_0^\infty \exp\left(T_e \eta^2 \nu^{\frac{\alpha}{2}} - 2\pi\lambda\beta\left(T_e, \alpha\right)\right)\right) \mathrm{d}\nu \end{aligned} \quad (18)$$

where $T_c = T_e = \frac{-\frac{\ln(5\beta_0)}{cP_c}\left(2^C - 1\right)}{\pi_c}$ and in SFR it receives interference from both the central cell user band as well as the cell edge user band with different powers, i.e. $I_x = \sum_{i \in I_{ii}} P_c d_{i,n})^{-\alpha} + \sum_{i \in I_{io}} P_e d_{i,n}^{-\alpha}$, if the user belongs to the central cell area and $I_x = \sum_{i \in I_{oi}} P_c d_{i,n}^{-\alpha} + \sum_{i \in I_{oo}} P_e d_{i,n}^{-\alpha}$, if the user belongs to cell edge area.

4.3 Strict FFR Coverage Probability Analysis

We define coverage probability as the probability that the users instantaneous SINR is greater than the value called SINR threshold. The coverage probability of FFR resource allocation scheme is given as follows,

$$P\left(\gamma_{n_q,q}\left(x_{n_q}\right) > \gamma_c \mid x\right) = P\left(\hat{h}_{n_q}^2 > a \mid x\right). \quad (19)$$

From the Appendix C, the coverage of the users belongs to the central cell area frequency band is given as

$$\begin{aligned} &P\left(\gamma_c\left(q\right) > \gamma_c \mid \epsilon(q) = \epsilon_c\right) \\ &= \int_0^\infty P\left(\gamma_{n_q,q}\left(x_{n_q}\right) > \gamma_c \mid x\right) f_X(x) \mathrm{d}x \\ &= \sum_{i=1}^{M} \rho_i \left(\int_0^\infty \exp\left(T_c \eta^2 \nu^{\frac{\alpha}{2}} - 2\pi\lambda\beta\left(T_c, \alpha\right)\right)\right) \mathrm{d}\nu \end{aligned} \quad (20)$$

where $\beta\left(T_c, \alpha\right) = \Gamma\left(-\frac{2}{\alpha}, \left[\frac{\gamma_c}{\pi_c P_c}\right]\right) - \Gamma\left(-\frac{2}{\alpha}\right)$ and $T_c = \frac{\gamma_c}{\pi_c P_c}$, respectively.

Similarly, for the users of the cell edge area frequency band is given as

$$\begin{aligned} &P\left(\gamma_e\left(q\right) > \gamma_c \mid \epsilon(q) = \epsilon_e\right) \\ &= \int_0^\infty P\left(\gamma_{n_q,q}\left(x_{n_q}\right) > \gamma_c \mid x\right) f_X(x) \mathrm{d}x \\ &= \sum_{i=1}^{M} \rho_i \left(\int_0^\infty \exp\left(T_e \eta^2 \nu^{\frac{\alpha}{2}} - 2\pi\lambda\beta\left(T_e, \alpha\right)\right)\right) \mathrm{d}\nu \end{aligned} \quad (21)$$

where $\beta\left(T_e, \alpha\right) = \Gamma\left(-\frac{2}{\alpha}, \left[\frac{\gamma_c}{\pi_c P_e}\right]\right) - \Gamma\left(-\frac{2}{\alpha}\right)$ and $T_e = \frac{\gamma_c}{\pi_c P_e}$ respectively.

4.4 Soft FFR Coverage Probability Analysis

Similarly, the coverage probability of SFR resource allocation scheme can be derived.

In the Appendix C, I_x represents the interference power. The only difference from strict FFR is this interference power. This is due to the use of frequency band of both the base stations corresponding to the central cell area users frequency band in the same power and the cell edge area users frequency band with different power. The coverage of the users belongs to the central cell area frequency band is given as

$$
\begin{aligned}
&P\left(\gamma_{\mathrm{c}}(q) > \gamma_{\mathrm{c}} \mid \epsilon(q) = \epsilon_{\mathrm{c}}\right) \\
&= \int_0^{\infty} P\left(\gamma_{n_q,q}\left(x_{n_q}\right) > \gamma_{\mathrm{c}} \mid x\right) f_X(x)\mathrm{d}x \\
&= \sum_{i=1}^{M} \rho_i \left(\int_0^{\infty} \exp\left(T_{\mathrm{c}}\eta^2 \nu^{\frac{\alpha}{2}} - 2\pi\lambda\beta\left(T_{\mathrm{c}}, \alpha\right)\right)\right) \mathrm{d}\nu
\end{aligned} \tag{22}
$$

where $\beta\left(T_{\mathrm{c}}, \alpha\right) = \Gamma\left(-\frac{2}{\alpha}, \left[\frac{\gamma_{\mathrm{c}}}{\pi_{\mathrm{c}} P_{\mathrm{c}}}\right]\right) - \Gamma\left(-\frac{2}{\alpha}\right)$ and $T_{\mathrm{c}} = \frac{\gamma_{\mathrm{c}}}{\pi_{\mathrm{c}} P_{\mathrm{c}}}$ respectively.

Similarly, for the users of the cell edge area frequency band is given as

$$
\begin{aligned}
&P\left(\gamma_{\mathrm{e}}(q) > \gamma_{\mathrm{c}} \mid \epsilon(q) = \epsilon_{\mathrm{e}}\right) \\
&= \int_0^{\infty} P\left(\gamma_{n_q,q}\left(x_{n_q}\right) > \gamma_{\mathrm{c}} \mid x\right) f_X(x)\mathrm{d}x \\
&= \sum_{i=1}^{M} \rho_i \left(\int_0^{\infty} \exp\left(T_{\mathrm{e}}\eta^2 \nu^{\frac{\alpha}{2}} - 2\pi\lambda\beta\left(T_{\mathrm{e}}, \alpha\right)\right)\right) \mathrm{d}\nu
\end{aligned} \tag{23}
$$

where $\beta\left(T_{\mathrm{e}}, \alpha\right) = \Gamma\left(-\frac{2}{\alpha}, \left[\frac{\gamma_{\mathrm{c}}}{\pi_{\mathrm{c}} P_{\mathrm{e}}}\right]\right) - \Gamma\left(-\frac{2}{\alpha}\right)$ and $T_{\mathrm{e}} = \frac{\gamma_{\mathrm{c}}}{\pi_{\mathrm{c}} P_{\mathrm{e}}}$ respectively.

5. Numerical Results

Different priorities such as spectral efficiency improvement and coverage probability may be given to the systems under various traffic loads and channel conditions. For example, the goal of networks experiencing high traffic loads is to improve the spectral efficiency. But, in another circumstance, the goal may be to improve the coverage probability of interference-limited cell edge area users.

In another scenario, peak data rates for the interference-limited edge users have to be improved. This section explores these tradeoffs and compares the performance of SFR and FFR using the Poisson model and proposes a resource allocation strategy for maximizing sum-rate as well as balancing resource efficiency based on traffic load.This section numerically evaluates the performance of the system.The performance of Strict FFR and Soft FFR are compared for the PPP model and also the effect of the FFR threshold (γ_{TH}) on the average spectral efficiency and coverage probability in the chunk-based Tractable Multi-cell OFDMA system are evaluated.

The algorithm steps to split the users into the central cell area users and the cell edge area users are described below:

- Step 1: In all cells, to calculate the SINR, the location is fixed at distance from the base station varied in step size of 50 m and angles are varied from 0 to 360 degrees at the step size of 5 degree.
- Step 2: At this location, SINR is calculated using distance between that point and desired base station point to calculate the desired power and that point to all the remaining base stations to calculate the interference power.

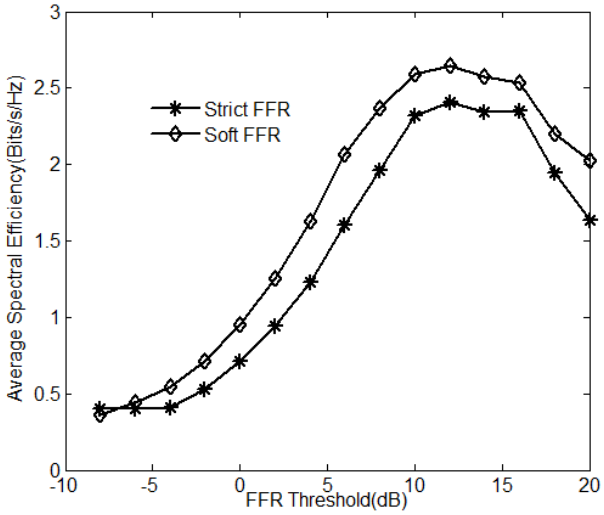

Fig. 4. Average spectral efficiency comparison.

- Step 3: Now, these calculated SINRs at every points are compared with FFR threhold. If SINR at the particular point reaches the FFR threshold, then that points are joined together to split the regions as the central cell area and cell edge area.The SINR circles are not concentric circle like hexagonal layout due to irregular cellular layout.
- Step 4: Step 3 was repeated for varying FFR threhold.
- Step 5: When FFR threshold is low, then SINR even at the edge may reach FFR threshold. Therefore, the whole cell is classified as the central cell area. Vice versa, if FFR threshold is large, then at no point the SINR reaches FFR threshold. Therefore, the whole cell is classified as the cell edge area.

After performing the cell area into the central area and edge cell, the frequency bands are allocated for FFR and SFR techniques using graph coloring as described in system model. The parameters taken to analyse the performance are listed in Tab. 1. The effect of the FFR threshold to split the users into the users of the central cell area and the users of the cell edge area on the average spectral efficiency in the chunk-based OFDMA system for tractable model is evaluated for both strict FFR and soft FFR resource allocation schemes. Also, the coverage probability comparison is made. The channel fading of each subcarrier for all the users is normalized and Rayleigh distributed with unitary mean square as illustrated in the system model. As described in Tab. 1, the coherence bandwidth, f_C, is five times of Δf, i.e.75 kHz. According to the equation (3) of [22], the correlation between adjacent subcarrier is high, when the channel coherence bandwidth is high. Also, the coherence bandwidth is taken in terms of subcarrier spacing. For the coherence bandwidth of $5\Delta f$, the correlation between adjacent subcarrier is 0.98. For this correlation, from the Fig. 5 of [22], the average spectral efficiency is better upto chunk size of 8. So, the chunk size was chosen as 8. The transmit power in the central cell area and cell edge area are first assumed as

Parameter	Value
Bandwidth	10 MHz
Number of subcarriers	600
Subcarrier spacing(Δf)	15 kHz
BER constraint(β_0)	10^{-3}
Coherence bandwidth	$5\Delta f$
Base station model	Poisson point process model

Tab. 1. Simulation parameters.

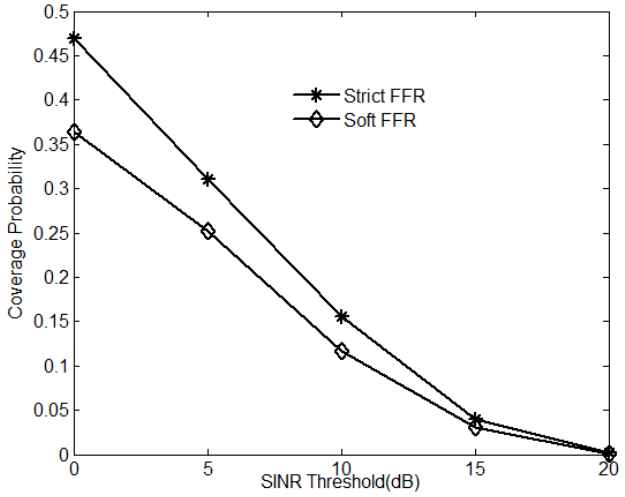

Fig. 5. Coverage probability comparison.

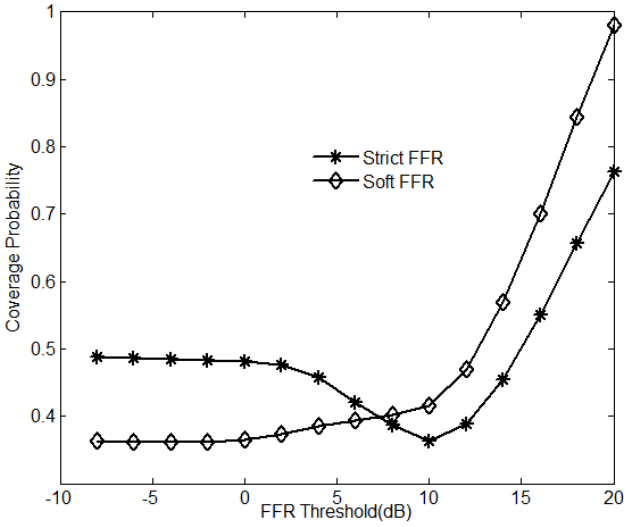

Fig. 6. Effect of FFR threshold γ_{TH} in coverage probability with SINR threshold = 0 dB.

the same, i.e. $P_{\mathrm{c}} = P_{\mathrm{e}}$. Reference to the literature BER constraint was taken as 10^{-3}.

Figure 4 shows the average spectral efficiency performance comparison between the FFR and SFR resource allocation methods. The average spectral efficiency increases as the FFR threshold up to the point called the optimal point. When FFR threshold is low, the probability of the users belongs to the central cell area frequency band is more. Even though the frequency reuse factor is high, this increases the interference power to the users which results in reduction in spectral efficiency. If FFR threshold gradually increases, then the number of the users of the cell edge area increases. Then the the users of the cell edge area are allocated with frequency band which does not receive more interference from all the base stations. After the optimal point, the average spectral efficiency starts decreasing with the FFR threshold.

At the optimal point of 12 dB for both Strict FFR as well as for Soft FFR, the probability of the number of users in the central cell area as well as the cell edge are approximately the same. So, the average efficiency is maximum at this optimal point. After the optimal point, the probability of the number of users in the cell edge area are high when compared to the users of the central cell area. This reduces interference. But, it also increases the use of frequency band with frequency reuse factor less than unity than frequency reuse factor 1. Also, from Fig. 4, as expected the spectral efficiency performance improvement is observed in SFR than in FFR. In SFR also, the users of the central cell area are high for low FFR threshold. Since the central cell area frequency band is not allocated to all the central cell area cells. But, the users with low received SINR also receives less interference than FFR. So, the spectral efficiency in SFR is better than FFR.

Figure 5 shows the performance comparison of resource allocation methods such as FFR and SFR from coverage probability point of view, when the transmitter power of the central cell and the cell edge area are the same. As expected, the coverage probability of both the schemes starts decreasing, when the SINR threshold increases. There is a gap in coverage probability between FFR and SFR resource allocation schemes, when the transmitter power in the central cell and the cell edge areas are the same. This occurred due to the allocation of the frequency band used in the users of the central cell area of one cell used by the cell edge area of adjacent cell area users.

Figure 6 shows the coverage probability comparison for varying FFR Threshold (dB) with SINR threshold of 0 dB. SFR performance is better, when the FFR threshold is low. The improvement in coverage probability performance is achieved, when the FFR threshold is greater than the optimal FFR threshold of 12 dB. Always, there is a trade-off between the average spectral efficiency performance and coverage probability, i.e. the average spectral efficiency starts decreasing after the optimal FFR threshold of 12 dB, but coverage probability starts increasing in all resource allocation schemes.

6. Conclusion

The base station locations have been modelled in this paper using Poisson Point Process to analyse the cellular in real environment. In order to reduce the complexity in the resource allocation scheme, chunk-based resource allocation has been embedded in the multi-cell tractable OFDMA environment. FFR and SFR methods have been implemented with chunk-based resource allocation. The average spectral efficiency and coverage probability performance analysis have been illustrated for these two methods and these two schemes have been compared. The optimal FFR threshold for both these resource allocation schemes is 12 dB. At this optimal value, the number of users in the central cell area of irregular cell and the cell edge area are the same. It is demonstrated that the SFR performance is better than FFR based resource allocation, when the spectral efficiency is considered. But, the numerical results confirmed that the coverage probability is poorer than FFR, when the transmitter power of central cell area and the users of the cell edge area are kept the same. Also, the trade-off between the spectral efficiency and coverage probability performance was observed in this paper.

Additionally, this work motivates future research for modern resource allocation method such as Soft-Partial Frequency Reuse(SPFR) to increase the capacity of the edge users and also to reduce the interference level i.e. hybrid of SFR and Partial Frequency Reuse (PFR) or FFR [32]. Also this research would allow research into the implications of FFR along with other important cellular network research including FFR in conjunction with Femto cell and sectoring to further improve the spectral efficency [33], [34].

References

[1] ASTELY, D., DAHLMAN, E., FURUSKAR, A., et al. LTE: The evolution of mobile broadband. *IEEE Communications Magazine*, 2009, vol. 47, no. 4, p. 44–51. DOI: 10.1109/MCOM.2009.4907406

[2] LI, G., LIU, H. Downlink radio resource allocation for multi-cell OFDMA system. *IEEE Transactions on Wireless Communication*, 2006, vol. 5, no. 12, p. 3451–3459. DOI: 10.1109/TWC.2006.256968

[3] POLAK, L., KALLER, O., KLOZAR, L., et al. Mobile communication networks and digital television broadcasting systems in the same frequency bands: Advanced co-existence scenarios. *Radioengineering*, 2014, vol. 23, no. 1, p. 375–386. ISSN: 1210-2512

[4] MILOS, J., POLAK, L., HANUS, S., et al. Wi-Fi influence on LTE downlink data and control channel performance in shared frequency bands. *Radioengineering*, 2017, vol. 26, no. 1, p. 201–210. DOI: 10.13164/re.2017.0201

[5] FOROUZAN, N., GHORASHI, S. Resource allocation for downlink Multi-Cell OFDMA cognitive radio network using hungarian method. *Radioengineering*, 2013, vol. 22, no. 4, p. 1117–1127. ISSN: 1210-2512

[6] GHAFFAR, R., KNOPP, R. Interference suppression strategy for cell-edge users in the downlink. *IEEE Transactions on Wireless Communications*, 2009, vol. 11, no. 1, p. 154–165. DOI: 10.1109/TWC.2011.111211.101921

[7] ALI, S. H., LEUNG, V. C. M. Dynamic frequency allocation in fractional frequency reused OFDMA networks. *IEEE Transactions on Wireless Communications*, 2009, vol. 8, no. 8, p. 4286–4295. DOI: 10.1109/TWC.2009.081146

[8] SOUMAYA, H., CHOONGIL, Y., JIHYUNG, K., et al. Dynamic hard fractional frequency reuse for Mobile WiMAX. In *Proceedings of the IEEE International Conference on Pervasive Computing and Communication*. 2009, p. 1-6. DOI: 10.1109/PERCOM.2009.4912869

[9] ZHU, H., KARACHONTZITIS, S., TOUMPAKARIS, D. Low-complexity resource allocation and its application to distributed antenna systems. *IEEE Wireless Communications*, 2010, vol. 17, no. 3, p. 44–50. DOI: 10.1109/MWC.2010.5490978

[10] ZHU, H., WANG, J. Chunk-based resource allocation in OFDMA systems- part I: Chunk allocation. *IEEE Transactions on Communications*, 2009, vol. 57, no. 9, p. 2734–2744. DOI: 10.1109/TCOMM.2009.09.080067

[11] PAPOUTSIS, V. D., KOTSOPOULOS, S. A. Chunk-based resource allocation in distributed MISO-OFDMA systems with fairness guarantee. *IEEE Communications Letters*, 2011, vol. 15, no. 4, p. 377–379. DOI: 10.1109/LCOMM.2011.020111.102273

[12] ZHU, H., WANG, J. Chunk-based resource allocation in OFDMA systems-part II: Joint chunk, power and bit allocation. *IEEE Transactions on Communications*, 2012, vol. 60, no. 2, p. 499–509. DOI: 10.1109/TCOMM.2011.112811.110036

[13] JUTHATIP, W., WIROONSAK, S. Chunk-based subcarrier assignment with power allocation and rate constraints for downlink OFDMA. In *Proceedings of the International Symposium on Communication and Information Technologies*. 2014, p. 494–498. DOI: 10.1109/ISCIT.2014.7011962

[14] SHEN, Z., ANDREWS, J. G., EVANS, B. L. Adaptive resource allocation in multiuser OFDM systems with proportional rate constraints. *IEEE Transactions on Wireless Communications*, 2005, vol. 4, no. 6, p. 2726–2730. DOI: 10.1109/TWC.2005.858010

[15] LI, J., SHROFF, N., CHONG, E. A reduced-power channel reuse scheme for wireless packet cellular networks. *IEEE/ACM Transactions Networking*, 1999, vol. 7, no. 6, p. 818–832. DOI: 10.1109/90.811448

[16] VARAHRAM, P., ALI, B. M. A low complexity partial transmit sequence for peak to average power ratio reduction in OFDM systems. *Radioengineering*, 2011, vol. 20, no. 3, p. 677–682. ISSN: 1210-2512

[17] CHRONOPOULOS, S. K., TATSIS, G., RAPTIS, V., et al. Enhanced PAPR in OFDM without deteriorating BER performance. *International Journal of Communications, Network and System Sciences*, 2011, vol. 4, p. 164–169. DOI: 10.4236/ijcns.2011.43020

[18] CHRONOPOULOS, S. K., CHRISTOFILAKIS, V., TATSIS, G., et al. Reducing peak-to-average power ratio of a Turbo coded OFDM. *Wireless Engineering and Technology*, 2012, vol. 3, p. 195–202. DOI: 10.4236/wet.2012.34028

[19] GAO, N., WANG, X. Optimal subcarrier-chunk scheduling for wireless OFDMA systems. *IEEE Transactions on Wireless Communications*, 2011, vol. 10, no. 7, p. 2116–2123. DOI: 10.1109/TWC.2011.050511.100458

[20] CHUNG, S. T., GOLDSMITH, A. J. Degrees of freedom in adaptive modulation: A unified view. *IEEE Transactions on Communications*, 2001, vol. 49, no. 9, p. 1561–1571. DOI: 10.1109/26.950343

[21] GONZALEZ, D., GARCIA-LOZANO, M., RUIZ, S., et al. An analytical view of static intercell interference coordination techniques in OFDMA networks. In *Proceedings of the IEEE Wireless Communications and Networking Conference*. 2012, p. 300–305. DOI: 10.1109/WCNCW.2012.6215510

[22] ZHU, H., WANG, J. Performance analysis of chunk-based resouynamicrce allocation in Multi-Cell OFDMA systems. *IEEE Journal on Selected Areas in Communications*, 2014, vol. 32, no. 2, p. 367–375. DOI: 10.1109/JSAC.2014.141216

[23] HAENGGI, M., ANDREWS, J. G., BACELLI, F., et al. Stochastic geometry and random graphs for the analysis and design of wireless networks. *IEEE Journal on Selected Areas in Communications*, 2009, vol. 27, no. 7 , p. 1029–1046. DOI: 10.1109/JSAC.2009.090902

[24] ANDREWS, J. G., BACCELLI, F., GANTI, R. K. A new tractable model for cellular coverage. In *Proceedings of the Allerton Conference on Communication, Control, and Computing*. 2010, p. 1204–1211. DOI: 10.1109/ALLERTON.2010.5707051

[25] GANTI, R. K., BACCELLI, F., ANDREWS, J. G. A new way of computing rate in cellular networks. In *Proceedings of the IEEE International Conference on Communications*. 2011, p. 1–5. DOI: 10.1109/icc.2011.5962727

[26] NOVLAN, T. D., GANTI, R. K., GHOSH, A., et al. Analytical evaluation of fractional frequency reuse for OFDMA cellular networks. *IEEE Transactions on Wireless Communications*, 2011, vol. 10, no. 12, p. 1–12. DOI: 10.1109/TWC.2011.100611.110181

[27] AHMED, J. Spectral efficiency comparison of OFDM and MC-CDMA with carrier offset. *Radioengineering*, 2017, vol. 26, no. 1, p. 221–226. DOI: 10.13164/re.2017.0221

[28] SUNG, N., STOYAN, D., KENDALL, et.al. *Stochastic Geometry and its Applications*. 3rd ed., John Wiley & Sons, 2013. ISBN: 978-0-470-66481-0

[29] ZHU, H., RAY LIU, K. J. *Resource Allocation for Wireless Networks: Basics, Techniques, and Applications*. 1st ed., Cambridge University Press, 2008. ISBN: 9780511619748

[30] CHANG, R., TAO, Z., ZHANG, J., et al. A graph approach to dynamic fractional frequency reuse (FFR) in multi-cell OFDMA networks. In *Proceedings of the IEEE International conference on Communications*. 2009, p. 1–6. DOI: 10.1109/ICC.2009.5198612

[31] SADR, S., ADVE, R. S. Partially-distributed resource allocation in small-cell networks. *IEEE Transactions on Wireless Communications*, 2014, vol. 13, no. 12, p. 6851–6862. DOI: 10.1109/TWC.2014.2327030

[32] GAJEWSKI, S. Soft- partial frequency reuse method for LTE-A. *Radioengineering*, 2017, vol. 26, no. 1, p. 359-368. DOI: 10.13164/re.2017.0359

[33] KAWSER, M. T., ISLAM, M. R., AHMED, K. I., et al. Efficient resource allocation and sectorization for fractional frequency reuse (FFR) in LTE femtocell systems. *Radioengineering*, 2015, vol. 24, no. 4, p. 940–947. DOI: 10.13164/re.2015.0940

[34] KAVITHA, P., SHANMUGAVEL, S. Spectral efficiency analysis of Multi-Cell OFDMA system with sectoring. *ICTACT Journal on Communication Technology*, 2017, vol. 8, no. 1, p. 1443–1446. DOI: 10.21917/ijct.2017.0213

About the Authors . . .

Pillappan KAVITHA was born in India, in 1979. She received the B.E. degree in Electronics and Communication Engineering from the Bharathidasan University, India, in 2002, and the M.E in Communication Systems from Thiagarajar College of Engineering, Madurai, India in 2009 and currently pursuing her Ph.D degree in Anna University, Chennai. She has 13 years of teaching experience. Her current research interests include cellular networks, MIMO-OFDM, probability and stochastic analysis etc. She is a Life member of the Indian Society for Technical Education (ISTE) and The Institute of Electronics, Information and Communication Engineers (IEICE).

Sethu SHANMUGAVEL received the B.Sc degree in Mathematics from the MK University, India, in 1975, and D.M.I.T in Electronics Engineering from MIT University, India, in 1978 and Ph.D. degrees in Coded Communication from Indian Institute of Technology, Kharagpur, West Bengal, India in 1989. He has more than 37 years of teaching experience. His current research interests include wireless communications, cognitive radio grid computing, etc. He has published more than 80 research papers in national and international journals and guided 18 Ph.D. scholars in the area of wireless communications, mobile ad hoc networks and ATM networks. He has also visited University of Central Florida, University of Illinois and Nebraska University in USA.

Appendix A

The average probability of q^{th} chunk assigned to the users in the central cell area,$P(\epsilon(q) = \epsilon_{\text{c}})$ is derived as follows

$$P(\epsilon(q) = \epsilon_{\text{c}}) = \sum_{N_{kc}=1}^{N_k} P(\epsilon(q) = \epsilon_{\text{c}} \mid N_{kc}) P(N_{kc}) \tag{24}$$

where $P(N_{kc})$ represents the probability of the number of users in the central cell area which is equal to N_{kc}. This can be derived as

$$P(N_{kc}) = \begin{pmatrix} N_k \\ N_{kc} \end{pmatrix} [P(\tilde{\gamma}_{kn} > \gamma_{\text{TH}})]^{N_{kc}} \, [1 - P(\tilde{\gamma}_{kn} > \gamma_{\text{TH}})]^{N_k - N_{kc}} \tag{25}$$

where $\begin{pmatrix} N_k \\ N_{kc} \end{pmatrix} = \frac{N_k!}{N_{kc}!(N_k - N_{kc})!}$ represents binomial coefficient. $P(\gamma_{kn} > \gamma_{\text{TH}})$ is the probability that a user located in the central cell area of the k^{th} cell, and $[1 - P(\gamma_{kn} > \gamma_{\text{TH}})]$ is the probability that a user located in the cell edge area. γ_{kn} is the average SINR of the user n in the k^{th}cell. Due to the assumption of uniform distribution of N_k users in the k^{th} cell, the probability that the n^{th} user located in the central cell area is obtained as follows.

The average received SINR of the user n is derived as

$$\hat{\gamma}_{kn} = E\left[\frac{P\hat{h}_{k,n,q}^2 x^{-\alpha}}{\sum_{i \in I} P_{\text{c}} d_{i,n}^{-\alpha} + \eta^2}\right], \tag{26}$$

$$\hat{\gamma}_{kn} = \frac{P x^{-\alpha}}{\sum_{i \in I} P_{\text{c}} d_{i,n}^{-\alpha} + \eta^2} \tag{27}$$

where $d_{i,n}$ is the distance between i^{th} base station and the corresponding user n. Equation (27) follows from (24) using $E[\hat{h}_{k,n,q}^2] = 1$, i.e. since, the sub channel is Rayleigh fading

with unitary mean square. Now, the average SINR is dependent on the distance, which is Poisson distributed random variable. So, $P(\gamma_{kn} > \gamma_{\mathrm{TH}})$ is derived as

$$\begin{aligned} P(\hat{\gamma}_{kn} > \gamma_{\mathrm{TH}}) &= P\left(\frac{Px^{-\alpha}}{\sum_{i\in I} P_{\mathrm{c}} d_{i,n}^{-\alpha}+\eta^2} > \gamma_{\mathrm{TH}}\right), \\ P(\hat{\gamma}_{kn} > \gamma_{\mathrm{TH}}) &= P\left(x < \left[\frac{P}{\gamma_{\mathrm{TH}}\left(\sum_{i\in I} P_{\mathrm{c}} d_{i,n}^{-\alpha}+\eta^2\right)}\right]^{\frac{1}{\alpha}}\right). \end{aligned} \tag{28}$$

Since base stations are located according Poisson distribution, (27) can be calculated as,

$$P(\hat{\gamma}_{kn} > \gamma_{\mathrm{TH}}) = \int_0^{\left[\frac{P}{\gamma_{\mathrm{TH}}\left(\sum_{i\in I} P_{\mathrm{c}} d_{i,n}^{-\alpha}+\eta^2\right)}\right]^{\frac{1}{\alpha}}} f_x(x)\mathrm{d}x \tag{29}$$

where $f_x(x) = 2\pi\lambda x \mathrm{e}^{-\lambda\pi x^2}$. So,

$$P(\hat{\gamma}_{kn} > \gamma_{\mathrm{TH}}) = 1-\exp\left(-\pi\lambda\left[\frac{P}{\gamma_{\mathrm{TH}}\left(\sum_{i\in I} P_{\mathrm{c}} d_{i,n}^{-\alpha}+\eta^2\right)}\right]^{\frac{2}{\alpha}}\right). \tag{30}$$

Assume,

$$\varepsilon = 1-\exp\left(-\pi\lambda\left[\frac{P}{\gamma_{\mathrm{TH}}\left(\sum_{i\in I} P_{\mathrm{c}} d_{i,n}^{-\alpha}+\eta^2\right)}\right]^{\frac{2}{\alpha}}\right). \tag{31}$$

Further, (23) can be written as

$$P(N_{kc}) = \binom{N_k}{N_{kc}} \varepsilon^{N_{kc}} [1-\varepsilon]^{N_k-N_{kc}}. \tag{32}$$

Substituting (10) and (32) in eq. (24), the probability that the q^{th} chunk allocated to the central cell area becomes as

$$P(\epsilon(q) = \epsilon_{\mathrm{c}}) = \sum_{N_{kc}=1}^{N_k} \binom{N_k}{N_{kc}} \varepsilon^{N_{kc}} [1-\varepsilon]^{N_k-N_{kc}} \left(\frac{N_{kc}}{N_k}\right). \tag{33}$$

Defining $n = N_{kc} - 1$, then (31) becomes

$$P(\epsilon(q) = \epsilon_{\mathrm{c}}) = \varepsilon \sum_{N_{kc}=1}^{N_k} \binom{N_k-1}{n} \varepsilon^{n} [1-\varepsilon]^{(N_k-1)-n}. \tag{34}$$

Since the sum $\sum_{N_{kc}=1}^{N_k} \binom{N_k-1}{n} \varepsilon^{n} [1-\varepsilon]^{(N_k-1)-n} = 1$, then equation (32) reduces to

$$P\left(\epsilon(q) = \epsilon_{\mathrm{c}}\right) = \varepsilon = 1-\exp\left(-\pi\lambda\left[\frac{P}{\gamma_{\mathrm{TH}}\left(\sum_{i\in I} P_{\mathrm{c}} d_{i,n}^{-\alpha}+\eta^2\right)}\right]^{\frac{2}{\alpha}}\right). \tag{35}$$

Appendix B

The probability distribution functions of $C_{\mathrm{c}}(q)$ and $C_{\mathrm{e}}(q)$ can be derived from the cumulative distribution function of the conditional data rate $r_{n,q}(x_n, \theta_n)$ [22], the CDF of $r_{n,q}(x_n, \theta_n)$ is given by

$$\begin{aligned} P(r_{n_q,q}(x_{n_q}, \theta_{n_q}) &= P\left(\log_2\left(1+\frac{c\gamma_{n_q,q}\left(x_{n_q},\theta_{n_q}\right)}{\ln(5\beta_0)}\right) < r\right), \\ P(r_{n_q,q}(x_{n_q}, \theta_{n_q}) &= P\left(\gamma_{n_q,q}\left(x_{n_q},\theta_{n_q}\right) < \frac{\ln(5\beta_0)}{c}\left(2^r-1\right)\right). \end{aligned} \tag{36}$$

Equation (36) follows from BER function $\beta \approx 0.2\exp\left(-\frac{1.6\gamma(x,\theta)}{l-1}\right)$. Here, adaptive QAM modulation was considered. In (36), β_0 is BER constraint, $c = -1.6$, since the SINR $\gamma_{n_q,q}(x_{n_q}, \theta_{n_q})$ is function of $\hat{h}^2_{1,n,q}$ of the n^{th} user, the probability density function of the sum of the M independent exponentially distributed random variables is given by

$$\begin{aligned} f_{\hat{h}^2_{1,n,q}}(x) &= \sum_{i=1}^{M} \frac{1}{\pi_i}\rho_i \exp\left(\frac{-x}{\pi_i}\right), \\ P(\hat{h}^2_{n_q} < a) &= \left[P(\hat{h}^2_{1,n,q} < a)\right]^N, \\ P(\hat{h}^2_{1,n,q} < a) &= E_d\left(P(\hat{h}^2_{1,n,q} < a) \mid x\right) \end{aligned} \tag{37}$$

where x is the distance between the base station and the corresponding user, which is Poisson distributed random variable.

$$\begin{aligned} P(\hat{h}^2_{1,n,q} < a) \mid x) &= \int_0^a f_{\hat{h}^2_{1,n,q}}(x)\mathrm{d}x \\ P(\hat{h}^2_{1,n,q} < a) \mid x) &= \sum_{i=1}^{M} \rho_i \left[1-\exp\left(\frac{-a}{\pi_i}\right)\right] \end{aligned} \tag{38}$$

The conditional probabilities $P(C_{\mathrm{c}}(q) < C \mid x)$ and $P(C_{\mathrm{e}}(q) < C \mid x)$ are derived as follows, $P(C_{\mathrm{c}}(q) < C \mid x) = P(r_{n_q,q}(x_{n_q}, \theta_{n_q}) < C \mid x)$. From (27), interference power $I_x = \sum_{i\in I} P_{\mathrm{c}} d_{i,n}^{-\alpha}$

$$P(C_{\mathrm{c}}(q) < C \mid x) = P\left(\hat{h}^2_{1,n,q} < \frac{\ln(5\beta_0)}{c}(2^C-1)\frac{I_x+\eta^2}{P_{\mathrm{c}}x^{-\alpha}} \mid x\right),$$

$$P(C_{\mathrm{c}}(q) < C \mid x) = E_{I_x}\left(\sum_{i=1}^{M}\rho_i\left[1-\exp\left(\frac{\frac{-\ln(5\beta_0)}{c}(2^C-1)\frac{I_x+\eta^2}{P_{\mathrm{c}}x^{-\alpha}}}{\pi_i}\right)\right]\right),$$

$$P(C_{\mathrm{c}}(q) < C \mid x) = \sum_{i=1}^{M}\rho_i\left[1-E_{I_x}\left(\exp\left(\frac{\frac{-\ln(5\beta_0)}{c}(2^C-1)\frac{I_x+\eta^2}{P_{\mathrm{c}}x^{-\alpha}}}{\pi_i}\right)\right)\right]. \tag{39}$$

Using equation (24) of [24], $E_{I_x}\left(\exp\left(\frac{\frac{-\ln(5\beta_0)}{c}(2^C-1)\frac{I_x+\eta^2}{P_{\mathrm{c}}x^{-\alpha}}}{\pi_i}\right)\right)$ is given as follows,

$$E_{I_x}\left(\exp\left(\frac{\frac{-\ln(5\beta_0)}{c}(2^C-1)\frac{I_x+\eta^2}{P_{\mathrm{c}}x^{-\alpha}}}{\pi_i}\right)\right) = \exp\left(\frac{\frac{-\ln(5\beta_0)}{c}(2^C-1)\frac{\eta^2}{P_{\mathrm{c}}x^{-\alpha}}}{\pi_i}\right) L_{I_x}\left(\frac{\ln(5\beta_0)(2^C-1)}{c\pi_i P_{\mathrm{c}}x^{-\alpha}}\right). \tag{40}$$

Equation (40) follows from the concept of where $L_{I_x}\left(\frac{\ln(5\beta_0)(2^C-1)}{c\pi_i P_c x^{-\alpha}}\right)$ is the Laplace transform. This is due to $E_x(e^{-sx}) = \int_0^\infty e^{-sx} f(x)dx$ = Laplace transform of $f(x)$. Defining $d_{i,n}$ as the distance between i^{th} base station and n^{th} user in the reference cell but identical distribution for all i, using the definition of Laplace transform, we can get,

$$\begin{aligned} &L_{I_x}(s) = E_{I_x}(\exp(-sI_x), \\ &L_{I_x}(s) = E_I\left(\exp\left(-s\textstyle\sum_{i\in I} d_{i,n}^{-\alpha}\right)\right), \\ &L_{I_x}(s) = E_I\left(\textstyle\prod_{i\in I}\exp\left(-sd_{i,n}^{-\alpha}\right)\right), \\ &L_{I_x}(s) = \exp\left(-2\pi\lambda\textstyle\int_x^\infty\left[1-\exp\left(-s\nu^{-\alpha}\right)\right]\nu d\nu\right). \end{aligned} \tag{41}$$

Equation (41) follows from the probability generating functional [24] of the PPP and [28]. Since the interfering base stations are at least at a distance of x, i.e. the distance between the user and the desired base station, the limit for integration takes from x to ∞. Substituting $\nu^{-\alpha} = y$, i.e. changing of variable and $s = \frac{\ln(5\beta_0)(2^C-1)}{c\pi_i P_c x^{-\alpha}}$, then the Laplace transform can be obtained as,

$$\begin{aligned} &L_{I_x}\left(\frac{\ln(5\beta_0)(2^C-1)}{c\pi_i P_c x^{-\alpha}}\right) = \\ &\exp\left(\pi\lambda x^2 - 2\pi\lambda\left[\frac{\ln\left(5\beta_0\right)\left(2^C-1\right)}{c\pi_i P_c}\right]^{\frac{2}{\alpha}}\right. \\ &\left.x^2\left(\Gamma\left(\frac{-2}{\alpha},\left[\frac{\ln\left(5\beta_0\right)\left(2^C-1\right)}{c\pi_i P_c}\right]\right)-\Gamma\left(\frac{-2}{\alpha}\right)\right)\right) \end{aligned} \tag{42}$$

Substituting (40) in (38), we obtain

$$\begin{aligned} &E_{I_x}\left(\exp\left(\frac{\frac{-\ln(5\beta_0)}{c}(2^C-1)\frac{I_x+\eta^2}{P_c x^{-\alpha}}}{\pi_i}\right)\right) = \\ &\left(\exp\left(\frac{\frac{-\ln(5\beta_0)}{c}(2^C-1)\frac{\eta^2}{P_c x^{-\alpha}}}{\pi_i}\right)\right)\exp\left(\pi\lambda x^2 - 2\pi\lambda\right. \\ &\left.\left[\frac{\ln(5\beta_0)(2^C-1)}{c\pi_i P_c}\right]^{\frac{2}{\alpha}} x^2\left(\Gamma\left(\frac{-2}{\alpha},\left[\frac{\ln(5\beta_0)(2^C-1)}{c\pi_i P_c}\right]\right)-\Gamma\left(\frac{-2}{\alpha}\right)\right)\right) \end{aligned} \tag{43}$$

Consider $T_c = \frac{\frac{-\ln(5\beta_0)}{cP_c}(2^C-1)}{\pi_i}$ and $\beta(T_c,\alpha) = [\frac{\ln(5\beta_0)(2^C-1)}{c\pi_i P_c}]^{\frac{2}{\alpha}}\left(\Gamma\left(\frac{-2}{\alpha},\left[\frac{\ln(5\beta_0)(2^C-1)}{c\pi_i P_c}\right]\right)-\Gamma\left(\frac{-2}{\alpha}\right)\right)$, then (40) becomes

$$\begin{aligned} &E_{I_x}\left(\exp\left(\frac{\frac{-\ln(5\beta_0)}{c}(2^C-1)\frac{I_x+\eta^2}{P_c x^{-\alpha}}}{\pi_i}\right)\right) = \\ &\exp\left(T_c x^{-\alpha}\eta^2 + \pi^2 - 2\pi\lambda\beta\left(T_c,\alpha\right), x^2\right). \end{aligned} \tag{44}$$

Substituting (44) in (39), then $P(C_c(q) < C \mid x)$ becomes

$$\begin{aligned} &P(C_c(q) < C \mid x) = \\ &\sum_{i=1}^{M}\rho_i\left[1-\exp\left(T_c x^{-\alpha}\eta^2 + \pi^2 - 2\pi\lambda\beta\left(T_c,\alpha\right), x^2\right)\right]. \end{aligned} \tag{45}$$

Similarly, $P(C_e(q) < C \mid x) = P\left(r_{n_q,r}\left(x_{n_q},\theta_{n_q}\right) < 4C \mid x\right)$

$$\begin{aligned} &P(C_e(q) < C \mid x) = \\ &\sum_{i=1}^{M}\rho_i\left[1-\exp\left(T_o x^{-\alpha}\eta^2 + \pi^2 - 2\pi\lambda\beta\left(T_e,\alpha\right), x^2\right)\right] \end{aligned} \tag{46}$$

where $T_e = \frac{\frac{-\ln(5\beta_0)}{cP_c}(2^C-1)}{\pi_i}$ and $\beta(T_e,\alpha) = \left[\frac{\ln(5\beta_0)(2^{4C}-1)}{c\pi_i P_c}\right]^{\frac{2}{\alpha}}\left(\Gamma\left(\frac{-2}{\alpha},\left[\frac{\ln(5\beta_0)(2^{4C}-1)}{c\pi_i P_c}\right]\right)-\Gamma\left(\frac{-2}{\alpha}\right)\right)$.

$P(C_c(q) < C)$ can be derived as

$$P(C_c(q) < C) = \int_0^\infty P(C_c(q) < C \mid x) f_x(x)dx. \tag{47}$$

Similarly, $P(C_e(q) < C)$ is given as

$$P(C_e(q) < C) = \int_0^\infty P(C_e(q) < C \mid x) f_x(x)dx \tag{48}$$

where $f_x(x) = 2\pi\lambda x e^{-\lambda\pi x^2}$.

Appendix C

The coverage probability of FFR resource allocation scheme can be derived as follows,

$$P(\gamma_{n_q.q}(x_{n_q}) > \gamma_C \mid x) = P(\hat{h}_{n_q}^2 > a \mid x). \tag{49}$$

From Appendix B, $P(\hat{h}_{n_q}^2 > a \mid x)$ can be obtained. If the user belongs to the central cell area, then

$$\begin{aligned} P\left(\hat{h}_{n_q}^2 > \gamma_C\frac{I_x+\eta^2}{P_c x^{-\alpha}} \mid x\right) &= E_{I_x}\left(\sum_{i=1}^{M}\rho_i\exp\left(\frac{-\gamma_C\frac{I_x+\eta^2}{P_c x^{-\alpha}}}{\pi_i}\right)\right) \\ &= \sum_{i=1}^{M}\rho_i E_{I_x}\left(\exp\left(\frac{-\gamma_C\frac{I_x+\eta^2}{P_c x^{-\alpha}}}{\pi_i}\right)\right), \end{aligned} \tag{50}$$

$$\begin{aligned} P\left(\hat{h}_{n_q}^2 > \gamma_C\frac{I_x+\eta^2}{P_e x^{-\alpha}} \mid x\right) &= E_{I_x}\left(\sum_{i=1}^{M}\rho_i\exp\left(\frac{-\gamma_C\frac{I_x+\eta^2}{P_e x^{-\alpha}}}{\pi_i}\right)\right) \\ &= \sum_{i=1}^{M}\rho_i E_{I_x}\left(\exp\left(\frac{-\gamma_C\frac{I_x+\eta^2}{P_e x^{-\alpha}}}{\pi_i}\right)\right). \end{aligned} \tag{51}$$

From Appendix B, the terms in the above Equations (48) and (49) are given as

$$\begin{aligned} &E_{I_x}\left(\exp\left(\frac{-\gamma_C\frac{I_x+\eta^2}{P_c x^{-\alpha}}}{\pi_i}\right)\right) = \exp\left(\frac{-\gamma_C\frac{\eta^2}{P_c x^{-\alpha}}}{\pi_i}\right)\exp\left(\pi\lambda x^2 -\right. \\ &\left.2\pi\lambda\left[\frac{\gamma_C}{\pi_i P_c}\right]^{\frac{2}{\alpha}} x^2\left(\Gamma\left(\frac{-2}{\alpha},\left[\frac{\gamma_C}{\pi_i P_c}\right]\right)-\Gamma\left(\frac{-2}{\alpha}\right)\right)\right), \end{aligned} \tag{52}$$

$$\begin{aligned} &E_{I_x}\left(\exp\left(\frac{-\gamma_C\frac{I_x+\eta^2}{P_e x^{-\alpha}}}{\pi_i}\right)\right) = \exp\left(\frac{-\gamma_C\frac{\eta^2}{P_e x^{-\alpha}}}{\pi_i}\right)\exp\left(\pi\lambda x^2 -\right. \\ &\left.2\pi\lambda\left[\frac{\gamma_C}{\pi_i P_e}\right]^{\frac{2}{\alpha}} x^2\left(\Gamma\left(\frac{-2}{\alpha},\left[\frac{\gamma_C}{\pi_i P_e}\right]\right)-\Gamma\left(\frac{-2}{\alpha}\right)\right)\right), \end{aligned} \tag{53}$$

$$P\left(\hat{h}_{n_q}^2 > \gamma_C \frac{I_x+\eta^2}{P_c x^{-\alpha}} \mid x\right) = \sum_{i=1}^{M} \rho_i \exp\left(\frac{-\gamma_C \frac{\eta^2}{P_c x^{-\alpha}}}{\pi_i}\right) \exp\left(\pi\lambda x^2\right) - 2\pi\lambda \left[\frac{\gamma_C}{\pi_i P_c}\right]^{\frac{2}{\alpha}} x^2 \left(\Gamma\left(\frac{-2}{\alpha}, \left[\frac{\gamma_C}{\pi_i P_c}\right]\right) - \Gamma\left(\frac{-2}{\alpha}\right)\right). \quad (54)$$

Similarly

$$P\left(\hat{h}_{n_q}^2 > \gamma_C \frac{I_x+\eta^2}{P_e x^{-\alpha}} \mid x\right) = \sum_{i=1}^{M} \rho_i \exp\left(\frac{-\gamma_C \frac{\eta^2}{P_e x^{-\alpha}}}{\pi_i}\right) \exp\left(\pi\lambda x^2\right) - 2\pi\lambda \left[\frac{\gamma_C}{\pi_i P_e}\right]^{\frac{2}{\alpha}} x^2 \left(\Gamma\left(\frac{-2}{\alpha}, \left[\frac{\gamma_C}{\pi_i P_e}\right]\right) - \Gamma\left(\frac{-2}{\alpha}\right)\right), \quad (55)$$

$$P(\gamma_c(q) > \gamma_C \mid \epsilon(q) = \epsilon_c)$$

$$= \int_0^\infty P\left(\gamma_{n_q,q}\left(x_{n_q} > \gamma_C \mid x\right)\right) f_x(x)\,\mathrm{d}x,$$

$$= \sum_{i=1}^{M} \rho_i \int_0^\infty \exp\left(T_c \eta^2 \nu^{\frac{\alpha}{2}} - 2\pi\lambda\beta\left(T_c, \alpha\right)\right) \mathrm{d}\nu. \quad (56)$$

Here, $\beta(T_c, \alpha) = \Gamma\left(\frac{-2}{\alpha}, \left[\frac{\gamma_C}{\pi_i P_c}\right]\right) - \Gamma\left(\frac{-2}{\alpha}\right)$ and $T_c = \frac{\gamma_C}{\pi_i P_c}$ respectively.

Similarly, for the users of the cell edge area

$$P(\gamma_e(q) > \gamma_C \mid \epsilon(q) = \epsilon_e)$$

$$= \int_0^\infty P\left(\gamma_{n_q,q}\left(x_{n_q} > \gamma_C \mid x\right)\right) f_x(x)\,\mathrm{d}x,$$

$$= \sum_{i=1}^{M} \rho_i \int_0^\infty \exp\left(T_e \eta^2 \nu^{\frac{\alpha}{2}} - 2\pi\lambda\beta\left(T_e, \alpha\right)\right) \mathrm{d}\nu. \quad (57)$$

Here, $\beta(T_e, \alpha) = \Gamma\left(\frac{-2}{\alpha}, \left[\frac{\gamma_C}{\pi_i P_e}\right]\right) - \Gamma\left(\frac{-2}{\alpha}\right)$ and $T_e = \frac{\gamma_C}{\pi_i P_e}$ respectively.